Int J Earth Sci (Geol Rundsch) (2008) 97:705–723
DOI 10.1007/s00531-007-0185-z

ORIGINAL PAPER

Post-collisional melting of crustal sources: constraints from geochronology, petrology and Sr, Nd isotope geochemistry of the Variscan Sichevita and Poniasca granitoid plutons (South Carpathians, Romania)

Jean-Clair Duchesne · Jean-Paul Liègeois · Viorica Iancu · Tudor Berza · Dmitry I. Matukov · Mihai Tatu · Sergei A. Sergeev

Received: 2 August 2006 / Accepted: 21 February 2007 / Published online: 21 March 2007

Abstract The Sichevita and Poniasca plutons belong to an alignment of granites cutting across the metamorphic basement of the Getic Nappe in the South Carpathians. The present work provides SHRIMP age data for the zircon population from a Poniasca biotite diorite and geochemical analyses (major and trace elements, Sr–Nd isotopes) of representative rock types from the two intrusions grading from biotite diorite to biotite K-feldspar porphyritic monzogranite. U–Pb zircon data yielded 311 ± 2 Ma for the intrusion of the biotite diorite. Granites are mostly high-K leucogranites, and biotite diorites are magnesian, and calcic to calc-alkaline. Sr, and Nd isotope and trace element data (REE, Th, Ta, Cr, Ba and Rb) permit distinguishing five different groups of rocks corresponding to several magma batches: the Poniasca biotite diorite (P_1) shows a clear crustal character while the Poniasca granite (P_2) is more juvenile. Conversely, Sichevita biotite diorite (S_1), and a granite (S_2*) are more juvenile than the other Sichevita granites (S_2). Geochemical modelling of major elements and REE suggests that fractional crystallization can account for variations within P_1 and S_1 groups. Dehydration melting of a number of protoliths may be the source of these magma batches. The Variscan basement, a subduction accretion wedge, could correspond to such a heterogeneous source. The intrusion of the Sichevita–Poniasca plutons took place in the final stages of the Variscan orogeny, as is the case for a series of European granites around 310 Ma ago, especially in Bulgaria and in Iberia, no Alleghenian granitoids (late Carboniferous—early Permian times) being known in the Getic nappe. The geodynamical environment of Sichevita–Poniasca was typically post-collisional of the Variscan orogenic phase.

Keywords Granite modelling · Diorite · Zircon dating · Getic nappe

J.-C. Duchesne (✉) · J.-P. Liègeois
Department of Geology, University of Liège,
Bat. B20, 4000 Sart Tilman, Belgium
e-mail: jc.duchesne@ulg.ac.be

J.-P. Liègeois
Department of Geology, Africa Museum, Tervuren, Belgium
e-mail: jean-paul.liegeois@africamuseum.be

V. Iancu · T. Berza
Geological Institute of Romania, Bucharest, Romania
e-mail: viancu@igr.ro

T. Berza
e-mail: berza@igr.ro

D. I. Matukov · S. A. Sergeev
Center of Isotopic Research,
All-Russian Geological Research Institute (VSEGEI),
74 Sredny prospect, 199106 St.-Petersburg, Russia
e-mail: Dmitry_Matukov@vsegei.ru

S. A. Sergeev
e-mail: Sergey_Sergeev@vsegei.ru

M. Tatu
Geodynamical Institute of Romanian Academy,
Bucharest, Romania
e-mail: mtatu@geodin.ro

Introduction

Granitic rocks are a major constituent of the earth crust and, in orogenic belts, are typical products of recycling processes. Their study thus offers a most promising opportunity to unravel the mechanism of magma formation and evolution in the deep crust, together with giving insight into the nature of the source rocks that are melted. The

compositions of the primary melts, however, are often blundered by fractionation processes and the occurrence of crystals entrained from source rocks or from cumulates formed in the early phases of differentiation. In regions where granites occur together with mafic rocks, a major role has been assigned to the basic magma either as a source of heat to trigger the melting process, or as a mixing or hybridization component. Moreover, several types of material can potentially act as source rocks of granitic magmas depending on their mineralogy, on the availability of fluids of various compositions, and on temperature. Finally, several sources can melt together, simultaneously with different degrees of melting, or in sequence along a PT path.

North and South of the Danube Gorges that cross the South Carpathians and separate Romania from Serbia, four major granitoid bodies cut across the basement of the Getic nappe, which is the most important Alpine nappe of the South Carpathians (Fig. 1). These bodies form a discontinuous alignment 100 km long and up to 10 km wide (Sandulescu et al. 1978), suggesting a continuous batholith buried beneath the Mesozoic and Cenozoic cover sequences. In Serbia (from south to north), the main plutons are known as the Neresnica and Brnjica plutons (Vaskovic and Matovic 1997; Vaskovic et al. 2004), the latter in direct continuation across the Danube river with the Sichevita pluton in Romania. A fourth granitoid pluton, 15 km north of the latter and separated by Mesozoic sediments, was named the Poniasca pluton by Savu and Vasiliu (1969).

The similarity in petrography, mineralogy and major element geochemistry of the Sichevita and Poniasca plutons supports the hypothesis of a geometrical continuity between the two Romanian plutons. Comparison with available data on the Serbian plutons is further pointing to the occurrence of a regional batholith. More detailed geochemical studies on the Romanian occurrences, including trace elements and Sr and Nd isotopes which are presented here, show, however, a more complex image. Both intrusions result from different crystallization processes and imply several magma types. Moreover, it is inferred that both plutons originated by partial melting of several distinct sources.

Geological framework of the granite intrusions

The South Carpathians represent a segment of the Alpine-Carpathian-Balkan fold-thrust belt, moulded against the Moesian Platform as a horse shoe, with an eastern E–W oriented part and a western N–S oriented part, in the Romanian Banat and Eastern Serbia province (Fig. 1b). Since Murgoci (1905) discovered the main nappe structure, many syntheses based on hundreds of studies have proposed complex and partly conflicting models (see the reviews of Berza 1997 and Iancu et al. 2005a).

The South Carpathians are viewed as a Cretaceous nappe pile (Iancu et al. 2005a and references therein), in tectonic contact with the Moesian Platform (Stefanescu 1988; Seghedi and Berza 1994). The uppermost Cretaceous nappes of the South Carpathians are the Getic and Supragetic nappes. They include both pre-Alpine metamorphic basement and Upper Paleozoic–Mesozoic sedimentary cover (Iancu et al. 2005b). The Sichevita, Poniasca, Neresnica and Brnjica plutons have intruded into the metamorphic basement of the Getic nappe. According to Iancu et al. (1988), Iancu and Maruntiu (1989) and Iancu (1998), the pre-Alpine basement of the Getic nappe in the Romanian Banat is made up of several lithotectonic units (Fig. 1), assembled in Variscan times as thrust sheets and composed of various sedimentary, volcanic and (ultra) mafic protoliths, metamorphosed in several low to medium-high grade episodes.

Late Variscan post-thrust folding of the getic nappe basement is well expressed by regional dome-shaped structures. The alignment of the granitic plutons, though conspicuous on a large scale (Fig. 1), is considered by Savu et al. (1997) and Iancu (1998) to be tectonically controlled either by a host anticline or by a transcurrent fault. Late Variscan, extension-related movements following the nappe stacking and folding could also be envisaged.

The Sichevita and Poniasca granitoids

Former studies on Sichevita were made by Birlea (1977), Stan et al. (1992), Stan and Tiepac (1994) and Iancu (1998), while Poniasca granitoids have received less attention (see references in Savu et al. 1997).

Both granitoid plutons were re-interpreted as composite intrusions crosscutting the Variscan nappe pile of the Getic basement, north of Danube (Iancu et al. 1996; Iancu 1998). Both granitoids and their metamorphic country rocks are sealed to the west by unconformable Upper Carboniferous-Permian continental deposits and Mesozoic covers (Fig. 1). They are crosscutting the Variscan nappe pile of the Getic metamorphic basement, which is made up of four units (Iancu 1998). The Nera unit is mainly composed of metasedimentary micaschists and gneisses. The Ravensca unit is made up of gneisses with mafic and ultramafic protoliths, metamorphosed in amphibolite and eclogite facies conditions and retrogressed in greenschist facies conditions. Different from these, the low-grade Paleozoic formations are mainly represented by metabasalts and metadolerites of ensialic, back-arc related origin (Maruntiu et al. 1996), with associated carbonate rocks and black shales (Buceava unit) or metapelites (Minis unit).

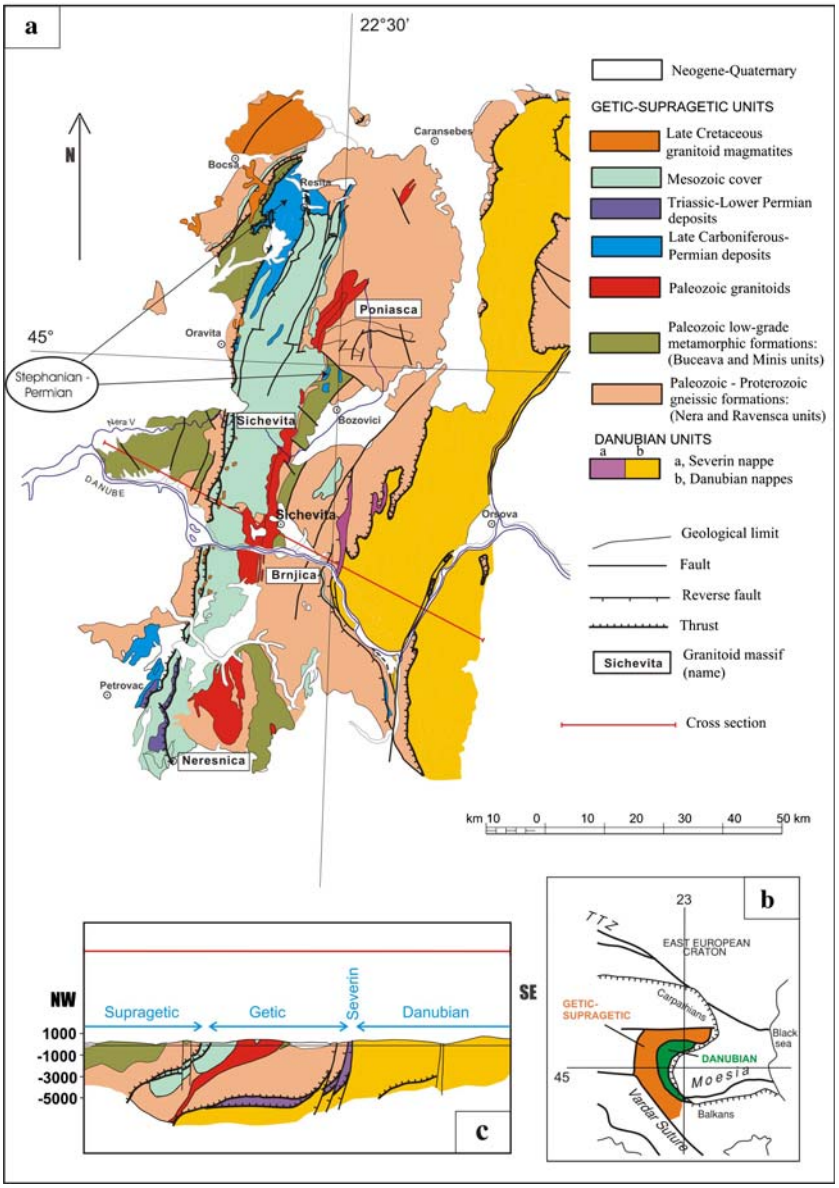

Fig. 1 **a** Generalised geological map of the Romanian Poniasca and Sichevita granites and related Serbian intrusions (modified after Sandulescu et al. 1978 and Iancu et al. 2005b). **b** Sketch map of the various geological units in the Carpathians belt; **c** Tentative cross-section through the geological units, parallel to the Danube river

Contact metamorphism of the studied granitoid plutons is marked by neoformation of biotite and andalusite (Savu et al. 1997) as well as of garnet and muscovite (Iancu 1998). Detailed mapping of the Poniasca pluton shows that the contacts are grossly parallel to a foliation in the surrounding gneisses (Savu et al. 1997). Locally, clear crosscutting relationships are observed with the foliation in the Ravesca unit. The round northern end of the pluton (Fig. 1) fits an antiform structure in the country rocks (Savu et al. 1997). The granitoids show a foliation parallel to the border, with microgranular dark enclaves and crystalline schist xenoliths elongated in the same plane. This foliation itself is crosscut by undeformed late pegmatitic and aplitic veins (see Fig. 4 in Savu et al. 1997). The observed magmatic planar flow structures inside both Sichevita and Poniasca plutons (Savu et al. 1997; Iancu 1998) could result from a syn-emplacement ballooning deformation of the intrusion.

North-East/South-West sub-vertical faults follow part of the eastern border of the Sichevita pluton and both the eastern and western borders of the Poniasca body. They sometimes contain thin concordant granitoid dykes and are marked by local low-temperature mylonites (actinolite-chlorite-albite schists). These faults and the elongation of the massifs suggest some kind of tectonic control (Iancu et al. 1996) on the emplacement in zones of apparent weakness parallel to the regional foliation and shear zones. Considering the structural features mentioned above and the Late-Variscan age of the plutons, the tectonic setting can be defined as post-collisional (Liégeois 1998).

Petrography of the Sichevita and Poniasca granitoids

The Sichevita and Poniasca granitoid plutons consist of a series of rocks intermediate between two major petrographic types: (1) hornblende biotite diorite, and (2) biotite K-feldspar porphyritic granite. The contacts between the two rock types are commonly sharp and lobated, giving evidence that both were intruded at the same time. Both rock types contain mafic magmatic enclaves (=MME; Didier and Barbarin 1991) or schlieren of dioritic composition, suggesting that mixing processes may have played an important role in the formation of intermediate compositions. In the present study, the biotite diorite will be named S_1 (for Sichevita) and P_1 (for Poniasca), and the biotite K-feldspar porphyritic granites will be defined S_2 and P_2, respectively.

(1) Biotite diorite

Biotite diorite (S_1, P_1) is a medium-to coarse-grained inequigranular massive rock, composed of plagioclase, biotite, hornblende, quartz, zircon, apatite, titanite, allanite and Fe–Ti oxides. K-feldspar is rarely present. Plagioclase ($An_{20–30}$) shows albite twinning and wavy oscillatory zoning, is anhedral and partially albitised or rimmed with albite. Dark brown biotite is present as inclusions in plagioclase, or as large interstitial crystals, containing zircon, apatite, zoned allanite and skeletal titanite. Green hornblende is common and always replaced by biotite. Epidote, chlorite, sericite and albite occur in deformed and altered samples.

(2) Biotite K-feldspar porphyritic granite

Biotite K-feldspar granite (S_2, P_2) is porphyritic, with variably rounded phenocrysts of poikilitic microcline perthite. The latter is rimmed by albite and may contain inclusions of plagioclase and small quartz grains, as well as fine-grained biotite and muscovite. Anhedral plagioclase ($An_{20–30}$), with strong oscillatory zoning, typically shows corroded rims of albite or microcline. Quartz is interstitial. Rare myrmekites develop at the contact between plagioclase and K-feldspar. Biotite is dark brown, mainly interstitial, and contains accessory phases (zircon, apatite, titanite and Fe–Ti oxides). It is replaced by white mica. Primary muscovite locally occurs in P_2 samples. Hornblende is rare in this petrographic type, but garnet is common. In rare deformed and altered samples, epidote, albite, chlorite, sericite and hematite are also present.

Geochronology

Published isotopic ages from the various outcrops definitely differ, but all point to Variscan events. For Sichevita granitoids, Birlea (1977) quotes 328–350 Ma U–Pb monazite ages (determined by Grünenfelder at ETH Zürich) and 250–310 Ma K–Ar microcline and biotite ages (determined by Tiepac at Nancy). In the Serbian Brnjica pluton, Rb–Sr ages of 259–272 Ma are reported by Vaskovic et al. (2004). A Carboniferous emplacement minimum age is in agreement with the presence of pebbles from the granitoid plutons in the Upper Carboniferous conglomerates exposed at the base of the unconformable sedimentary cover.

A biotite diorite from the Poniasca pluton is dated here using the U–Pb on zircon chronometer. Eleven zircon grains from sample#1 (R4710) were analysed (Table 1). The measurements were carried out on a SHRIMP-II ion microprobe at the Centre for Isotopic Research (VSEGEI, St. Petersburg, Russia; for methodology see Appendix).

The zircon crystals are zoned and may have relic cores (Fig. 2a–d). Two cores were analysed and give older ages than the outer rims. One core (6.1, Fig. 2c) is nearly concordant (3% discordant) and its $^{207}Pb/^{206}Pb$ age is 891 ± 20 Ma; the other core (5.2, Fig. 2c) is more strongly discordant and no meaningful age can be calculated on this single grain. Within the other nine zircon crystals, seven measurements determine a Concordia age of 311 ± 2 Ma (2σ; MSWD= 0.06; Fig. 2e). The two remaining zoned zircon crystals (4.1 and 5.1; Fig. 2b and 2c) are also concordant but at a slightly older age of 324 ± 4 Ma ($2\ \sigma$; MSWD= 0.84). Taken together, the 11 zircon analyses define a discordia with an upper intercept at 895 ± 56 Ma and a lower intercept at 319 ± 14 Ma.

The emplacement of the Poniasca pluton is precisely dated at 311 ± 2 Ma by magmatic zircons or magmatic overgrowths on inherited zircons. Although based only on a few core analyses, the $^{207}Pb/^{206}Pb$ age of 891± 20 Ma (Fig. 2e, inset) can be considered either as the age of the source of the magma (inherited zircon grain), or at least of a major contaminant of the diorite magma. The position of the core 5.2 in the Concordia diagram (Fig. 2e) is considered as the result of Pb loss of a ca. 890 Ma old zircon during the Poniasca magmatic event. The concordant fractions giving the 324 ± 4 Ma age are interpreted as being inherited from an early partial melting event. The main conclusions are that the intrusion of the Poniasca pluton (and by correlation also of the Sichevita pluton) occurred at 311± 2 Ma. These granitoids are contemporaneous to the Variscan granites on the other side of the Moesian platform, i.e. the San Nikola calc-alkaline granite at 312 ± 4 Ma and the Koprivshtitsa two-mica leucocratic granite at 312 ± 5 Ma (Carrigan et al. 2005). As is the case in Bulgaria, this puts the Poniasca-Sichevita plutons on the young side of the European post-collisional magmatism that are predominantly 340–320 Ma old (see review in Carrigan et al. 2005). In addition, at least the dated biotite

Table 1 SHRIMP ages for zircon from rock R4710 (sample#1) from the Poniasca intrusion

Spot	$\%^{206}Pb_c$	ppm U	ppm Th	$^{232}Th/^{238}U$	ppm $^{206}Pb^*$	$^{206}Pb^*/^{238}U$ Age	$^{207}Pb^*/^{206}Pb$ Age	% Dis	$^{207}Pb^*/^{206}Pb^*$	±%	$^{207}Pb^*/^{235}U$	±%	$^{206}Pb^*/^{238}U$	±%	err corr
R4710.1.1	0.04	273	107	0.40	11.6	312.4 ± 2.8	345 ± 59	9	0.05340	2.6	0.3650	2.8	0.04965	0.93	0.336
R4710.2.1	0.28	381	170	0.46	16.4	313.4 ± 2.7	293 ± 76	−7	0.05220	3.3	0.3580	3.4	0.04982	0.88	0.256
R4710.3.1	0.10	366	156	0.44	15.9	317.5 ± 2.8	247 ± 64	−29	0.05110	2.8	0.3560	2.9	0.05049	0.91	0.311
R4710.4.1	0.10	345	135	0.40	15.3	324 ± 2.8	257 ± 49	−26	0.05140	2.2	0.3650	2.3	0.05154	0.90	0.386
R4710.5.1	0.21	223	88	0.41	9.87	323.1 ± 3.4	291 ± 130	−11	0.05210	5.8	0.3690	5.9	0.05140	1.10	0.179
R4710.5.2	0.01	658	250	0.39	34.1	378 ± 2.8	457 ± 31	17	0.05612	1.4	0.4672	1.6	0.06039	0.77	0.486
R4710.6.1	0.05	366	201	0.57	45.3	866.2 ± 6.6	891 ± 20	3	0.06873	0.96	1.3630	1.3	0.14380	0.81	0.647
R4710.6.2	0.08	1202	194	0.17	50.5	307.4 ± 2.5	297 ± 33	−3	0.05227	1.4	0.3520	1.6	0.04884	0.82	0.500
R4710.6.3	0.06	322	47	0.15	13.5	307.3 ± 2.8	270 ± 50	−14	0.05160	2.2	0.3477	2.4	0.04883	0.93	0.395
R4710.7.1	0.06	260	106	0.42	10.9	305.7 ± 2.8	292 ± 76	−5	0.05220	3.3	0.3490	3.5	0.04857	0.94	0.273
R4710.8.1	0.14	365	148	0.42	15.6	312.8 ± 2.6	424 ± 54	26	0.05530	2.4	0.3790	2.6	0.04971	0.85	0.331

Errors are 1-sigma; Pb_c and Pb^* indicate the common and radiogenic portions, respectively. *% Dis* % of discordance

Error in standard calibration was 0.35%. Pb*= radiogenic lead (common Pb corrected using measured ^{204}Pb)

diorite contains old material whose age is 891 ± 20 Ma, an age also known from zircon cores in Bulgarian orthogneisses of Variscan age (Carrigan et al. 2006).

Geochemistry

Major element geochemistry

The Ponisaca and Sichevita plutons were extensively studied by Romanian petrologists and a large amount of analyses are available (Savu and Vasiliu 1969; Savu et al. 1997; Birlea 1976; Stan et al. 1992; Iancu et al. 1996). In this study, representative samples of the main petrographic types were collected in the field (Table 2), and analysed for major elements (XRF), trace elements (ICP-MS) and isotopes (TIMS). The methods are briefly described in the appendix. The new major element data (Table 3) are compared to the former analyses in Figs. 3, 4. The various element contents form continuous trends from ca. 60 to 75% SiO_2, i.e. from biotite diorite to granite. The trends are roughly linear and point to a second group of rocks, made up by mafic microgranular inclusions (sensu Didier and Barbarin 1991). It is shown by Figs. 3, 4 that our sample selection covers reasonably well the interval of composition of the Romanian samples from biotite diorite to granite. The mafic microgranular inclusions were not re-studied because of exceptional occurrence. The calc-alkaline character already noted by Iancu et al. (1996) of the composite series is confirmed in the AFM diagram (Fig. 4) in which the samples show a linear trend with little variation in the Fe/Mg ratio. The granites (Table 3) have high silica contents and are slightly peraluminous (ASI: 0.96–1.13). Their normative quartz and feldspar contents are above 95% (except#8 at 92%), which indicates leucogranitic compositions. In the classification of Frost et al. (2001), they show calcic to alkali-calcic compositions in the modified alkali-lime index (MALI) and are magnesian to ferroan. In the K_2O versus SiO_2 diagram (Peccerillo and Taylor 1976) the samples have a medium- to high-K composition.

In the Harker diagram for Na_2O (Fig. 3) the large dispersion of the data points may result from the late albitisation process revealed by the petrographical study. The dispersion of some K_2O values (Fig. 3) can also be explained by a late metasomatic alteration. In particular, the high K_2O content of the mafic enclaves suggests interdiffusion of K between the granitic and the basic melts. Crystallization of biotite in the basic melt could have maintained the K content in the melt at a low value, thus promoting exchange of K with the granitic melt (see the review by Debon 1991). If the two mobile elements Na and K are excluded, the linear trends observed for the immobile

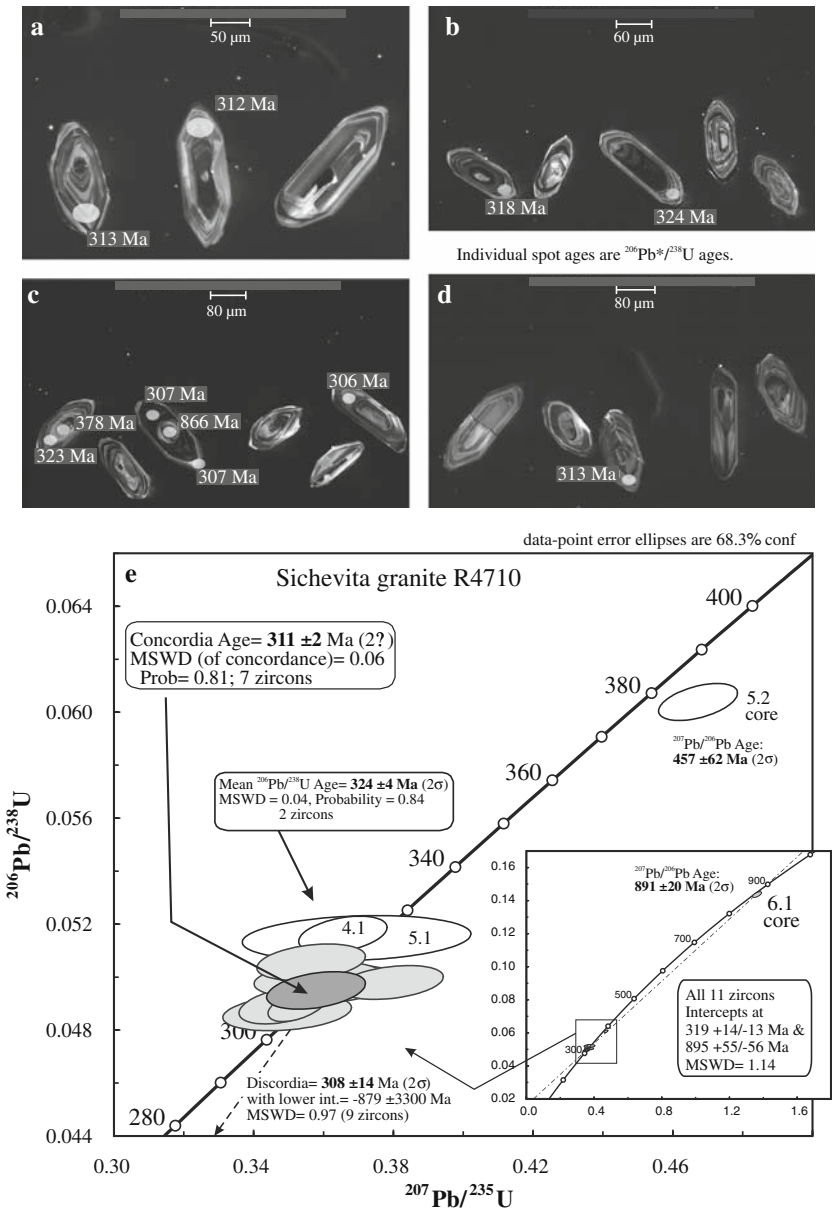

Fig. 2 Geochronological data on zircon grains from the Poniasca biotite diorite R4710 (sample#1). **a**–**d** Location of the analysed spots on zircon grains. **e** U–Pb concordia diagram for the various analysed zircon spots shown in photos (**a**)–(**d**) (see text)

elements (Fe, Ti, Mg, Al) suggest that a mixing process has played a fundamental role in the differentiation of the igneous rocks. This could have occurred by hybridization between basic and granitic magmas (Fenner 1926), or a granitic melt carrying solid source material as enclaves and/or individual crystals (the restite model of Chappell et al. 1987 and Chappell and White 1991). These working hypotheses are however not tenable when the trace element contents and isotopic compositions are considered.

Trace element variation

Trace element data are given in Table 3 and their variations are displayed in Figs. 5, 6. Except for Zr and Co, no linear trends between two poles are observed, precluding mixing processes (Fig. 5). Diorite from Sichevita body (S_1) and from Poniasca body (P_1) can be distinguished by their Cr and Ba contents, which are higher in P_1. REE in P_1 (Fig. 6b; Table 3) have higher La/Yb ratios (16–29) than in samples 5 and 4 from S_1 (Fig. 6a), and two biotite diorites from S_1 (#7 and 6) have high La/Yb ratios (33–40) and concave upward HREE contents (Fig. 6a). The granite from Poniasca (P_2) is distinctly enriched in Rb and Ta compared to Sichevita (S_2) (Fig. 5). REE in the S_2 (including sample S_2*) and P_2 groups (Fig. 6c, d) display distributions with negative Eu anomalies, flat HREE patterns and variable La/Sm ratios.

Table 2 Location of the samples analysed in this work

Sample #	Type	Rock#	Location	
1	P1	R4710	Pusnicu brook:	Right side tributary of Poniasca valley, 1,500 m from confluence
2	P1	R4720	Poniasca valley	Source area, 10 km N from Poniasca valley with Minis river
3	P1	R365	Pusnicu brook	Right side tributary of Poniasca valley, 1,200 m from confluence
4	S1	R363	Danube-left bank	300 m East of Liuborajdea confluence with Danube
5	S1	R4628	Gramensca valley	Western branch of Sichevita basin, 5 km N from Sichevita village
6	S1	R364	Danube-left bank	250 m East of Liborajdea confluence with Danube
7	S1	R4626	Gramensca valley	100 m Downstream from 4628 sample
8	S2	R4663D	Liuborajdea valley	Left side tributary of Danube, sourse area, 4 km NW of Sichevita village
9	S2	R4636	Danube-left bank	2 km West of the Liuborajdea confluence with Danube
10	S2	R4636A	Danube-left bank	50 m East from sample 4636
11	S2*	R4658	Gramensca valley	400 m Downstream from 4628 sample
12	P2	R366	Poniasca valley	2,500 m Upstream from Poniasca-Minis confluence

Rb–Sr and Sm–Nd isotopes

Isotope analyses are given in Table 4. The isotopic ratios are recalculated to the zircon age of 311 Ma. The Rb–Sr data do not define an isochron, only an errorchron with a very high MSWD can be obtained (308 ± 55 Ma, initial $^{87}Sr/^{86}Sr$ (Sr_i) = 0.7060 ± 0.0015; MSWD = 371; 9 WR, not shown). However, the fact that the age obtained is close to the inferred intrusion age indicates that the Sr initial ratios are most probably primary. This is confirmed by the isochron that can be calculated when using only the Poniasca pluton (290 ± 28 Ma, Sr_i = 0.70787 ± 0.00030, MSWD = 2.8, 4 WR; not shown). Although based on only four points and a rather high MSWD, this isochron confirms the validity of the Sr initial ratios.

The Sm–Nd chronometer provides no meaningful ages, due to the small spread of the $^{147}Sm/^{144}Nd$ ratios. Single-stage T_{DM} model ages vary between 800 and 1,650 Ma for rocks having $^{147}Sm/^{144}Nd < 0.15$, giving a mean T_{DM} of 1,148± 1,75 Ma. Considering that the variability of the Sm/Nd ratios are mostly due to the magmatic evolution, two-stage T_{DM} model ages (T_{DM2}) have been calculated, using the $^{147}Sm/^{144}Nd$ ratio of the rock from present to 311 Ma, and an average crust value of 0.12 (Millisenda et al. 1994) beyond 311 Ma. This reduces the model age variation between 843 and 1,368 Ma, with a mean of 1,160± 1,18 Ma. The similarity of the two means (single-stage and two-stage T_{DM} model ages) supports the validity of the single-stage T_{DM} (T_{DM1}) model ages, when calculated with proper precision (± 100 Ma). However, the T_{DM2} model ages suggest two groups; one rather homogeneous with the older T_{DM2} in the 1320–1370 Ma range (groups P_1 and S_2) and the other with younger T_{DM2} between 840 and 1090 Ma (P_2 and group $S_1 + S_2$*). The sample dated by the zircon U-Pb method (#1, P_1) and bearing an 891 Ma old zircon core has a T_{DM1} of 1300 Ma and a T_{DM2} of 1360 Ma.

The ε_{Nd} and $^{87}Sr/^{86}Sr$ values, recalculated at 311 Ma, are plotted in Fig. 7. The diagram confirms the existence of two groups of biotite diorite. S_1 biotite diorites have ε_{Nd} values between 0 and –1 (T_{DM2}: 930–1,000 Ma) and can be considered as the samples with the most important juvenile component; P_1 biotite diorites have more negative ε_{Nd} values between –4 and –5.5 (T_{DM2}: 1,320–1,370 Ma) together with higher initial $^{87}Sr/^{86}Sr$ ratios, thus pointing to a greater input of an old crustal source. S_2 granites can be subdivided into a group with a crustal signature (low ε_{Nd} and relatively high initial $^{87}Sr/^{86}Sr$ ratio; T_{DM2}: 1,330–1,360 Ma) similar to P_1 diorites and one sample (#11, S_2*) with a more juvenile character (T_{DM2}: 840 Ma). P_2 granite is also distinctly more juvenile than the P_1 group. The dated sample (#1) has a low ε_{Nd} value (–5.4). Thus, the isotope ratios not only confirm the occurrence of two groups of biotite diorite (P_1 and S_1) but also show that the Poniasca granite (P_2) can be distinguished from S_2 granites, and that one sample of granite (S_2*) can be identified within the S_2 group. Paradoxically, in the Poniasca pluton, the granite appears less contaminated by crustal material than the biotite diorites, and in the Sichevita intrusion the granite S_2* is also more juvenile or less contaminated than the biotite diorites S_1. As a whole, the isotopic data suggest a heterogeneous crustal source or variable contaminations by an old crust of the Sichevita–Poniasca magmas.

Before discussing the implications of the subdivision of the rocks into different groups, it is necessary to discuss the variations within the groups and particularly within S_1 and S_2, in which a substantial interval of variations is observed.

Table 3 Major and trace element composition of representative samples from the Sichevita and Poniasca plutons

Sample#	1	2	3	4	5	6	7	8	9	10	11	12
Type	P1	P1	P1	S1	S1	S1	S1	S2	S2	S2	S2*	P2
Rock#	R4710	R4720	R365	R363	R4628	R364	R4626	R4663D	R4636	R4636A	R4658	R366
Major elements (%)												
SiO_2	60.41	62.59	65.77	62.22	64.56	66.94	68.73	71.16	73.60	75.18	73.55	73.33
TiO_2	0.68	0.64	0.60	0.82	0.67	0.61	0.44	0.29	0.18	0.02	0.15	0.07
Al_2O_3	17.75	17.32	14.59	17.34	16.12	14.65	15.85	14.81	13.60	14.17	14.19	14.38
Fe_2O_3t	5.84	5.27	4.49	4.66	4.11	3.72	3.29	2.56	1.75	0.04	1.59	0.93
MnO	0.07	0.06	0.05	0.1	0.08	0.08	0.06	0.04	0.02	0.01	0.05	0.09
MgO	4.05	2.61	2.16	2.04	2.17	1.83	1.42	1.08	0.69	0.19	1.44	0.04
CaO	4.84	4.68	4.62	4.63	4.63	3.28	3.81	1.97	1.55	0.59	1.37	0.82
Na_2O	2.85	3.28	4.09	4.45	4.31	5.13	3.62	3.90	3.03	5.14	4.47	4.55
K_2O	2.29	1.94	2.40	2.15	1.97	2.29	2.04	4.02	3.93	4.75	3.33	4.11
P_2O_5	0.2	0.16	0.19	0.16	0.13	0.19	0.08	0.08	0.07	0.04	0.04	0.05
LOI	1.41	1.61	1.54	1.66	1.48	1.83	0.93	0.86	0.89	0.93	0.79	1.35
Total	100.39	100.16	100.50	100.23	100.23	100.55	100.27	100.77	99.32	101.09	100.97	99.72
Trace elements (%)												
U	1.7	1.3	1.3	3.8	2.6	3.2	2.1	1.9	4.7	4.5	4.3	1.6
Th	8.2	11.1	9.8	3.1	5.3	7.4	7.4	18.8	15.7	4.4	10.7	5.4
Zr	255	267	231	198	188	133	145	103	92	37	81	38
Hf	7.0	7.3	6.0	4.9	4.6	3.2	3.6	3.3		1.4	2.9	1.7
Nb	9.6	8.9	6.6	10.6	10.8	6.8	8.7	12.4	11.6	10.00	11.1	12.2
Ta	0.4	0.5	0.3	0.9	0.8	0.7	0.3	0.8	1.1	1.5	1.4	2.8
Rb	82	79	83	89	75	85	75	119	129	136	129	212
Sr	433	447	416	459	414	332	395	199	169	91	157	119
Rb/Sr	0.19	0.18	0.20	0.19	0.18	0.26	0.19	0.60	0.76	1.49	0.82	1.78
Cs	2.3	3.8	3.5	7.1	3.2	5.1	3.0	3.2	3.7	2.1	4.6	15.5
Ba	1026	981	1173	521	492	558	478	782	596	389	501	345
Ba/Sr	2.4	2.2	2.8	1.1	1.2	1.7	1.2	3.9	3.5	4.3	3.2	2.9
K/Rb	233	205	239	200	219	224	227	282	253	288	215	161
K/Ba	19	16	17	34	33	34	35	43	55	102	55	99
V	111	100		67	64		46	29	19			
Cr	291	184		10	68		59	20	12	3		
Zn	63	56	48	61	60	53	49	30	30	9	41	40
Ni	25	22	14	9	16	8	9	2	bdl	bdl	bdl	bdl
Co	15	14	10	12	10	10	7	4		3	3	0
Cu	20	19	16	11	21	13	9	7	6	5	6	6
Ga	20	21	18	18	17	19	16	17	18	14	16	19
Pb	7	7	7	14	15	14	11	20	24	41	27	35
Y	14.8	10.7	8.5	16.4	15.9	5.9	3.7	34.6	26.3	21.9	16.0	14.9
La	36.1	51.1	34.1	13.5	17.8	37.3	24.3	35.0	24.7	7.9	19.1	9.2
Ce	66.5	92.1	69.8	28.9	35.8	73.6	41.0	74.0	50.7	18.0	36.1	20.6
Pr	8.1	10.7	7.8	3.6	4.0	7.3	4.4	8.6	5.6	2.0	3.8	2.2
Nd	31.8	36.8	27.7	14.7	15.9	23.9	15.5	30.2	20.6	7.1	13.3	7.9
Sm	6.00	5.54	4.67	4.08	3.69	3.38	2.11	6.40	4.88	2.02	2.98	2.33
Eu	1.81	1.73	1.53	1.22	1.16	0.92	0.91	0.92	0.73	0.31	0.50	0.43
Gd	4.22	3.93	3.24	3.61	3.51	2.32	1.32	5.38	4.50	2.31	2.46	2.07
Tb	0.57	0.48		0.52	0.51		0.16			0.47	0.52	0.42
Dy	2.95	2.29	1.86	2.97	2.98	1.28	0.75	5.55	4.22	3.22	2.68	2.42

Table 3 continued

Sample#	1	2	3	4	5	6	7	8	9	10	11	12
Type	P1	P1	P1	S1	S1	S1	S1	S2	S2	S2	S2*	P2
Rock#	R4710	R4720	R365	R363	R4628	R364	R4626	R4663D	R4636	R4636A	R4658	R366
Ho	0.63	0.47		1.80	0.60		0.14		0.95	0.71	0.61	0.53
Er	1.46	1.12	0.83	1.62	1.64	0.62	0.35	3.16	2.52	2.02	1.50	1.28
Tm	0.21	0.14		0.25	0.23		0.06		0.39	0.30	0.25	0.20
Yb	1.49	1.26	0.76	1.51	1.64	0.73	0.39	2.79	2.53	2.14	1.50	1.38
Lu	0.22	0.16	0.14	0.24	0.24	0.13	0.09	0.43	0.36	0.30	0.21	0.18
[La/Yb]n	16	26	29	6	7	33	40	8	6	2	8	4
Eu/Eu*	1.1	1.1	1.2	1.0	1.0	1.0	1.6	0.5	0.5	0.4	0.5	0.6
MALI	0.30	0.54	1.87	1.97	1.65	4.14	1.85	5.95	5.41	9.30	6.43	7.84
Fe*	0.56	0.65	0.65	0.67	0.63	0.65	0.68	0.68	0.70	0.17	0.50	0.95
ASI	1.14	1.10	0.84	0.98	0.93	0.89	1.06	1.04	1.13	0.96	1.06	1.07
Agp	0.40	0.43	0.64	0.56	0.57	0.74	0.51	0.73	0.68	0.95	0.77	0.83
$Na_2O + K_2O$	5.14	5.22	6.49	6.60	6.28	7.42	5.66	7.92	6.96	9.85	7.80	8.66
T sat zircon	814	820	777	776	770	739	772	744	817	688	730	677
T sat apatite	869	870	924	865	870	936	866	890	902	876	851	869

Fe*= FeOt/FeOt+MgO, MALI = $Na_2O + K_2O$-CaO (modified alkali-lime index of Frost et al. 2001), ASI = $Al_2O_3/Na_2O + K_2O + CaO–3.3P_2O_5$ (mol%),

Agp = $Na_2O + K_2O/Al_2O_3$ (mol%): T sat zircon: zircon saturation temperature after Watson and Harrison (1983), T sat apatite: apatite saturation temperature after Harrison and Watson (1984) bdl: below detection limit

Discussion

Modelling the biotite diorite and granite differentiation processes

Biotite diorite

In S_1 group, samples#5 and#4 have similar major and trace element contents, including nearly identical REE distributions (Fig. 5a). They have been averaged and labelled Dio in Fig. 8. Biotite diorite#7 displays a quite different REE distribution with a higher La/Yb ratio, an upward concave shape of the HREE and a positive Eu anomaly (Fig. 5a), and thus could represent a cumulate. It is thus interesting to examine whether this rock has any geochemical relationship with the average biotite diorite.

We have performed a mass balance calculation to define the composition of the cumulate that has to be extracted from the average biotite diorite Dio to produce rock#7. The composition of the various minerals used in the calculation (Table 5) is taken from the classical model of Martin (1987) on the differentiation from biotite diorite to granodiorite. Note that the total Fe and Mg contents are grouped in this model as a first approximation on the partitioning of Fe/Mg ratio between cumulate and melt. The chemical and modal compositions of the dioritic cumulate is given in Table 6 and the liquid line of descent resulting from its extraction from average diorite is graphically represented on Fig. 8. The agreement with the observed evolution is reasonably good. The modal composition of the cumulate is used to calculate the bulk partition coefficients (D) for trace elements using the mineral/melt distribution coefficients compiled after Martin (1987) and given in Table 7. A simple Rayleigh fractionation model ($c_L = c_O F^{D-1}$, in which c_O is the concentration in the parent liquid,c_L the concentration in the residual liquid and$F$ the fraction of residual liquid) is then calculated for several values of F. The results of this modelling for the REE are shown on Fig. 9a. It can be seen that the agreement is good; the increase in the LREE, the Eu anomaly, the concave upward shape of the HREE distribution and the high La/Yb ratio are closely simulated for $F = 0.65$. The model thus shows that a fractional crystallisation relationship between a less evolved average diorite and rock#7 is a likely process.

The higher REE contents of sample#6 (Fig. 6a) can be accounted for by adding a small amount of apatite (ca 1%) to sample#7. Because apatite does not strongly fractionate the HREE and LREE (Table 7), except for Eu which has a lower partition coefficient than Sm and Gd, the addition of apatite increases the REE and decreases the Eu anomaly, but without changing the slope of the distribution. The three Poniasca biotite diorites resemble sample#6, especially sample#3, and display slight positive Eu anomalies. They can be interpreted as having the same origin as the Sichevita diorites.

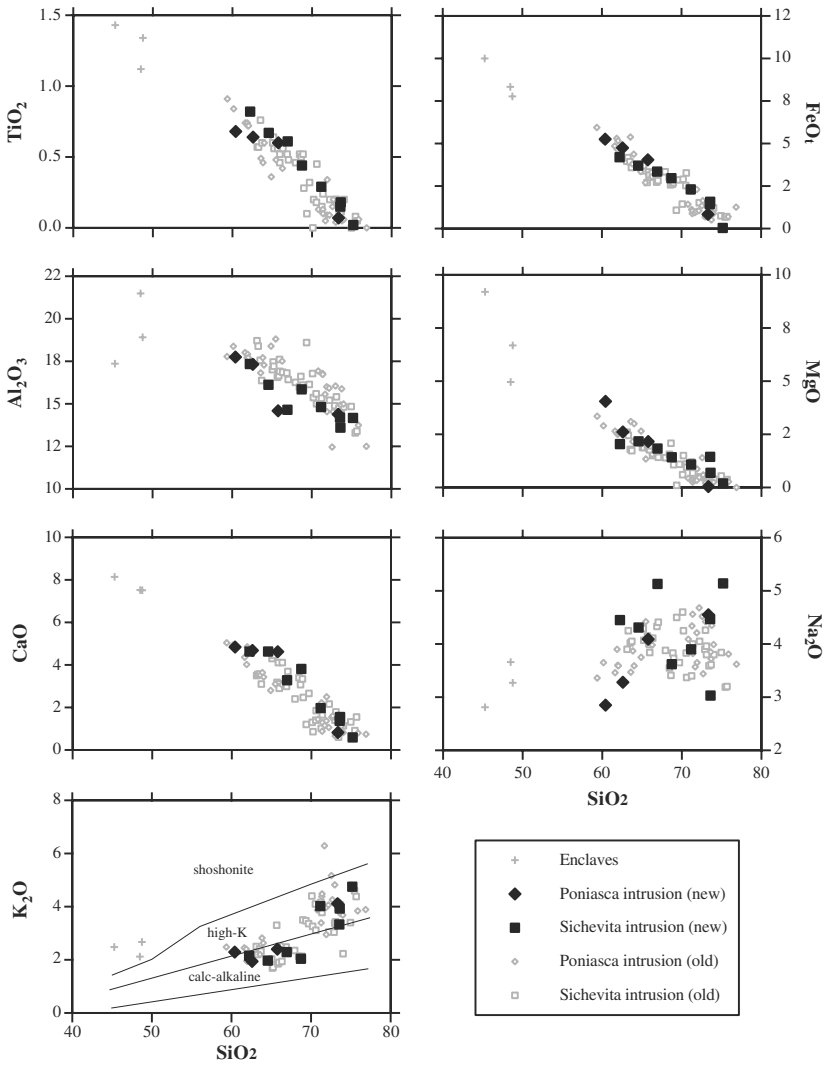

Fig. 3 Sichevita and Poniasca granite compositions plotted in Harker diagrams showing previous analyses (*open symbols*) and new analyses from this work (*closed symbols*). Data for the Poniasca granite are from Savu and Vasiliu (1969) and for the Sichevita granite from Birlea (1976) and Stan et al. (1992). New analyses from Table 3. In the K_2O vs. SiO_2 diagram, boundaries are from Peccerillo and Taylor (1976)

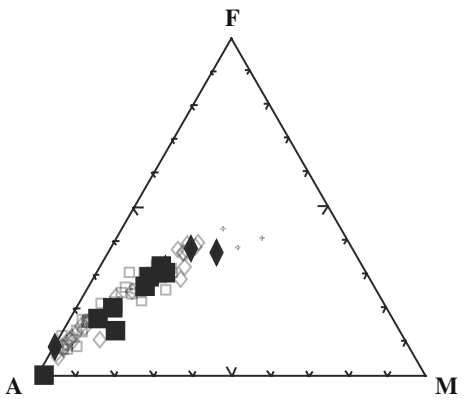

Fig. 4 Sichevita and Poniasca granite compositions plotted in AFM ($Na_2O + K_2O$, FeO_t, MgO) diagram. Same symbols and data sources as in Fig. 3

Granitoid

Modelling of the S_2 granitoids follows the same lines as for biotite diorite. Mass balance calculation (Tables 5 and 6) constrains the modal composition of the cumulate extracted from sample#8 which has the lowest SiO_2 content amongst the granitoids. The model is then used to calculate a composition similar to sample#9 which has the highest SiO_2 content (Fig. 8). For the trace elements, it is nevertheless necessary to subtract small amounts of accessory minerals which are most certainly at the liquidus of the granitic melt but occur in too small amounts to influence the major element balance. Indeed saturation temperatures for apatite and zircon (Watson and Harrison 1983; Harrison and Watson 1984) in sample#8 are 866°C and 744°C, respectively (Table 3), values that are most likely above the solidus temperature. Figure 9b displays the results of the REE modelling. The agreement between calculation

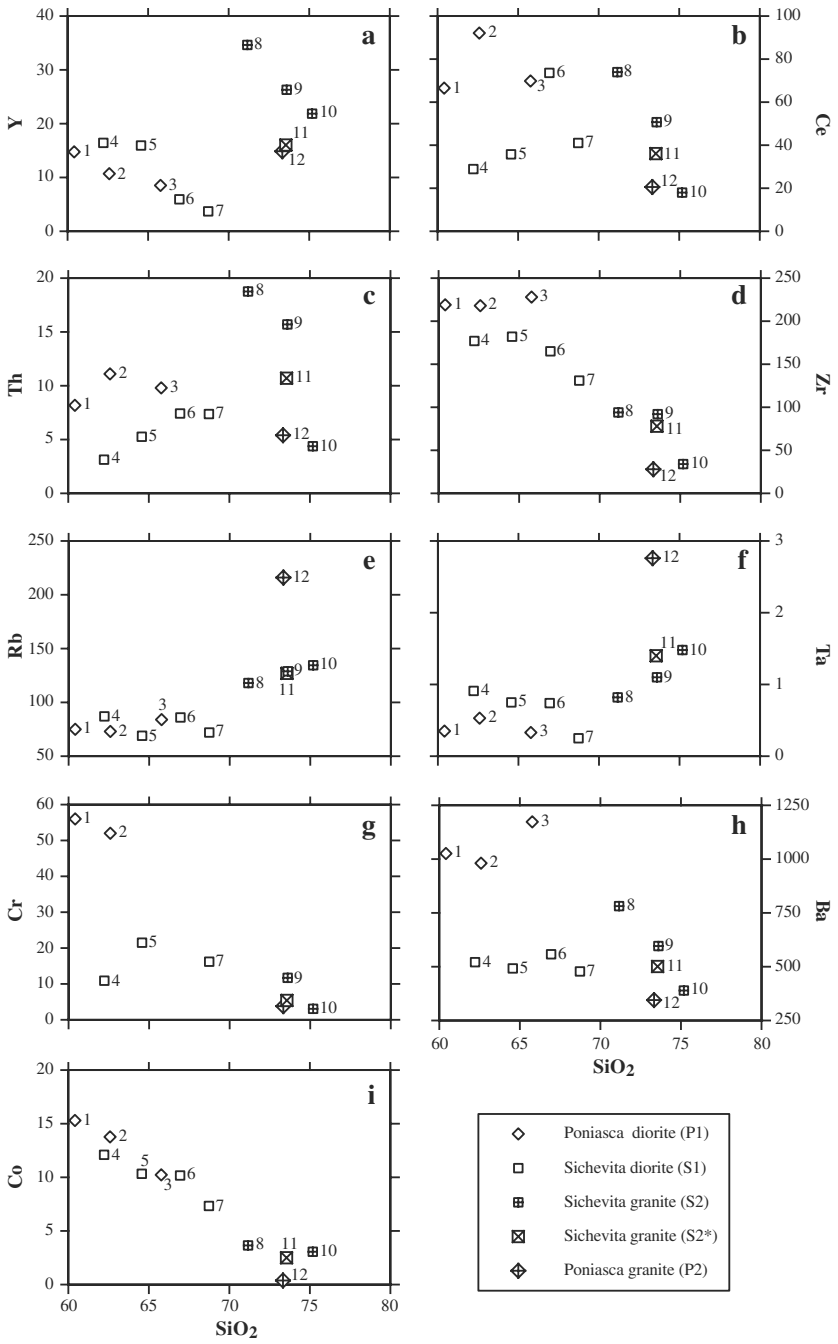

Fig. 5 Selected trace element compositions plotted in Harker diagrams. Data from Table 3

and observation is very good for F= 0.80. Again geochemistry corroborates the field and petrographic genetic relationships between the S_2 group samples.

The resemblance in major and trace element geochemistry of sample#11 (S_2*) with the S_2 group probably indicates that the mechanism of formation and the nature of the source were similar, except from an isotopic point of view. As for sample #12 (P_2), the enrichment in Rb and Ta remains intriguing; more data are needed to explain these features.

Relationships between diorites and granites

The geochemical modelling presented above for the Sichevita intrusion shows that the S_1 and S_2 groups together with sample S_2* can be considered as having crystallised from three distinct magma batches with different isotopic signatures, thus coming from different sources and evolving separately. However, it is interesting to explore an alternative hypothesis in which the S_1 and S_2 groups would be related by some contamination process. Figure 7 indeed

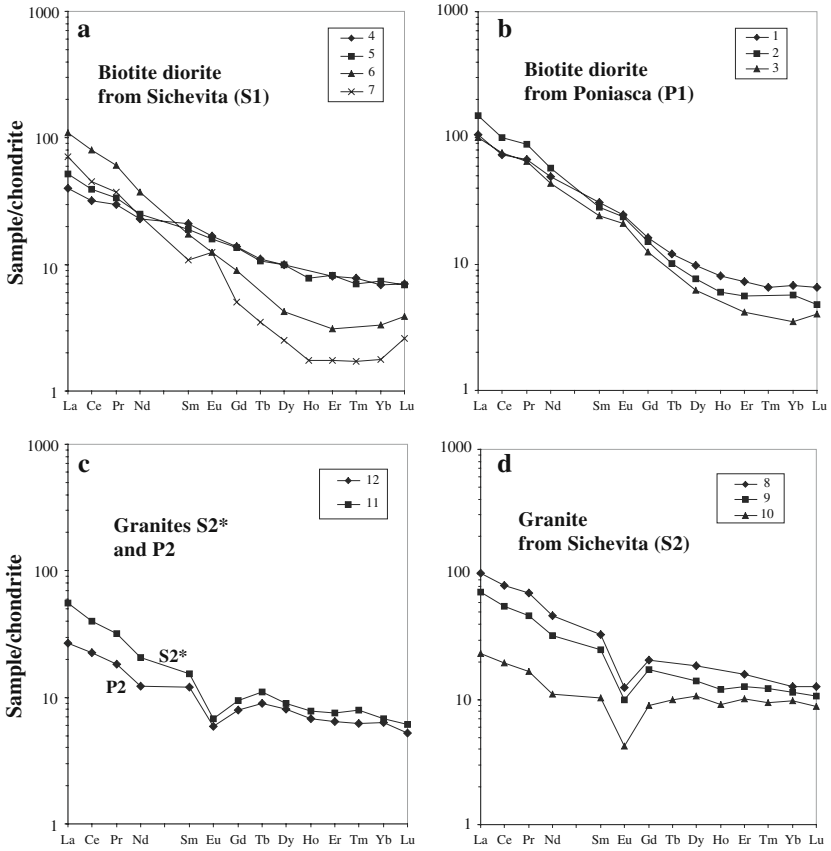

Fig. 6 Chondrite-normalised REE distribution in the Sichevita and Poniasca granites (data from Table 3). **a** Biotite diorite from Sichevita intrusion (S_1); **b** Biotite diorite from Poniasca intrusion (P_1); **c** Sichevita granite#11 (S_2*) and Poniasca granite #12 (P_2); and **d** Granite from Sichevita intrusion (S_2)

shows that the S_2 group can be isotopically related to S_1 group by a contamination process with an old crustal material with low ε_{Nd} values and high $^{87}Sr/^{86}Sr$ ratios. This possibility is not precluded by the major element compositions. Figure 8 shows that it is possible to pass from the most evolved diorite (sample #7; 69% SiO_2) to the less evolved granite (sample#8; 71% SiO_2) by adding a granitic component (> 71% SiO_2, > 4% K_2O). A more constraining condition, however, comes from the HREE distribution (Figs. 5a, 6a, d). The issue is to smooth off the upward concavity of the HREE distribution of sample#7 and obtain the REE content of sample#8 which is comparable to the average upper crust (ca. 30 ppm La and $[La/Yb]_n$ ratio ca. 10—Taylor and McLennan 1985). A simple calculation shows that mixing 20% of granitic material with REE contents three times higher than the average upper crust to sample#7 produces a composition in reasonable agreement with that of sample#8. A contaminant with such high REE contents is not common but exists (e.g. in REE-rich charnockititc rocks, Duchesne and Wilmart 1997). The process, however, requires a significant and unusual heat capacity of the diorite for either melting or assimilation. It is thus considered as possible but unlikely.

For the Poniasca intrusion, the major and trace element composition of the granitic melt (P_2) could possibly be derived from the biotite diorite (P_1) by grossly the same fractional crystallization and assimilation processes as those calculated for the Sichevita differentiation (Figs. 5 and 6). This scenario is however difficult to validate when the isotopes are considered. The P_2 sample has indeed a more juvenile character than the P_1 diorites, which would imply contamination with an unlikely granitic component with a positive ε_{Nd} value and a low $^{87}Sr/^{86}Sr$ ratio (Fig. 7).

It thus emerges from this modelling that both plutons were built up by two distinct batches of magma in the Poniasca intrusion and most probably three different batches were emplaced in the Sichevita pluton. These batches emplaced simultaneously (mingling relationship) but could have evolved separately, except maybe in zones at the contact between the magmas where some exchange between the melts could have taken place.

Variability of the sources of the Sichevita–Poniasca intrusions

The formation of dioritic melts through melting of metabasaltic material has been experimentally demonstrated by a number of authors (e.g. Helz 1976; Beard and Lofgren 1991; Rushmer 1991; Rapp and Watson 1995). The nature of the protolith can be identified by considering the major

Table 4 Rb–Sr and Sm–Nd isotopic compositions of rocks from the Sichevita and Poniasca plutons. Two-stage Nd T_{DM} model ages have been calculated with the $^{147}Sm/^{144}Nd$ ratio of the rock from present to 311 Ma, and with a $^{147}Sm/^{144}Nd$ ratio = 0.12 (average crust) beyond 311 Ma.

Group	Rock#	Rb ppm	Sr ppm	$^{87}Rb/^{86}Sr$	$^{87}Sr/^{86}Sr$	2σ	$(^{87}Sr/^{86}Sr)_{311\ Ma}$	Sm ppm	Nd ppm	$^{147}Sm/^{144}Nd$	$^{143}Nd/^{144}Nd$	2σ	(ε_{Nd})	$(^{143}Nd/^{144}Nd)_{311\ Ma}$	$(\varepsilon_{Nd})_{311\ Ma}$	T_{CHUR}	$T_{DM\ (DP)}$ 1-stage	$T_{DM\ (DP)}$ 2–*stage*
P1	1	R4710	81.6	433	0.546	0.710037	0.000013	0.707621	6.00	31.8	0.1142	0.512193	0.000011	–8.68	0.511960	–5.41	823	1301	1357
P1	2	R4720	78.7	447	0.510	0.710025	0.000010	0.707769	5.54	36.8	0. 0911	0.512170	0.000008	–9.13	0.511985	–4.94	676	1087	1323
P1	3	R365	83.3	416	0.580	0.710297	0.000011	0.707730	4.67	27.7	0.1020	0.512164	0.000008	–9.25	0.511956	–5.49	763	1199	1368
S1	4	R363	89.3	459	0.563	0.707276	0.000008	0.704784	4.08	14.7	0.1683	0.512525	0.000011	–2.20	0.512182	–1.08	607	1727	1007
S1	5	R4628	74.6	414	0.521	0.706629	0.000010	0.704322	3.69	15.9	0.1406	0.512516	0.000010	–2.38	0.512230	–0.15	332	1100	932
S1	6	R364	84.8	332	0.739	0.708537	0.000010	0.705266	3.38	23.9	0.0856	0.512373	0.000009	–5.17	0.512199	–0.76	364	804	981
S1	7	R4626	74.7	395	0.548	0.707158	0.000008	0.704734	2.11	15.5	0.0825	0.512370	0.000009	–5.23	0.512202	–0.69	358	789	976
S2	8	R4663D	118.5	199	1.724	0.714545	0.000014	0.706913	6.40	30.2	0.1282	0.512229	0.000009	–7.98	0.511968	–5.26	911	1447	1349
S2	9	R4636	128.9	169	2.205	0.715909	0.000014	0.706150	4.88	20.6	0.1432	0.512270	0.000007	–7.18	0.511979	–5.06	1047	1663	1332
S2	10	R4636A	136.0	91	4.333	0.726992	0.000007	0.707815	2.02	7.1	0.1716	0.512310	0.000008	–6.40	0.511961	–5.41	1988	2695	1361
S2*	11	R4658	128.5	157	2.378	0.714243	0.000009	0.703720	2.98	13.3	0.1356	0.512562	0.000008	–1.48	0.512286	0.95	190	944	843
P2	12	R366	212.2	119	5.171	0.729225	0.000009	0.706338	2.33	7.9	0.1798	0.512498	0.000009	–2.73	0.512132	–2.06	1258	2470	1087

and minor element contents of the biotite diorite, as suggested, e.g. by Jung et al. (2002). In the present case, the low TiO_2 content (< 1%), and the MgO content between 2 and 4% point to dehydration melting of basaltic compositions (Beard and Lofgren 1991; Rapp and Watson 1995), and the K_2O content below 2.5% refers to a medium-K composition (Roberts and Clemens 1993). The minimum melting temperatures of the biotite diorites, based on the saturation temperature of apatite (Harrison and Watson 1984) are in the 865–936°C range (Table 3). The isotopic compositions indicate two different sources for the Poniasca P_1 and Sichevita S_1 biotite diorites. The latter, with values close to bulk earth at 311 Ma, can represent a juvenile source; the former, with more evolved values, could represent a melting product of a contaminated juvenile source, or of an older crustal source. This suggestion is sustained by the presence of 891 Ma-old zircon cores in the dated biotite diorite (Fig. 2).

As for the Sichevita granite S_2, an anatectic origin by melting metasedimentary rocks (see, e.g. Chappell and White 1974; Pitcher 1987; Frost et al. 2001) is straightforward. The variation in the modified alkali lime index (MALI) values could reflect differences in water pressure at the time of melting (Holtz and Johannes 1991). The less evolved melt (#8) shows a relatively low Rb/Sr ratio (0.60) and Ba/Sr ratio (4), which suggests that biotite was present in the melting residue. A vapour-absent muscovite limited melting process (McDermott et al. 1996) can account for the high K_2O content. The isotope signature for the Poniasca and Sichevita granitic melts points to a crustal source, but sample#11 (S_2*), with a slightly positive ε_{Nd} value and a low Sr isotope ratio (0.7035) requires a source enriched in juvenile material. Apatite saturation temperatures (Table 3) in the granites are in the 850–900°C range, thus slightly lower than in the biotite diorites.

Both granitoids plutons are cutting across Variscan thrust sheets which cannot represent the source material of the magmas. To the N–E of the region, however, the Getic metamorphic basement comprises metasediments, eclogites, ultramafic-mafic bodies, etc., which are all strongly deformed, suggesting an accretion complex containing both oceanic and continental materials (Sabau and Massone 2003). This could represent a heterogeneous source analogous to that of the Sichevita–Poniasca plutons.

Geodynamical setting

Metamorphic peak conditions in the Getic metamorphic basement were dated in eclogites, peridotites and amphibolites at 358–323 Ma (Rb–Sr on minerals, Dragusanu and Tanaka 1999), at 358–341 Ma (Rb–Sr, Medaris et al. 2003) and at 338–333 Ma on a synkinematic pegmatite (U–Pb on single crystal zircons, Ledru et al. 1997). The

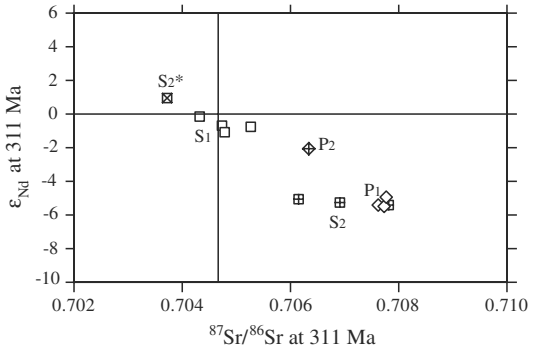

Fig. 7 ε_{Nd} vs. Sr isotope ratio at 311 Ma for samples from the Sichevita and Poniasca intrusions. Same symbols as in Fig. 5. Data in Table 4

Table 5 Major element compositions of the minerals used for mass balance calculations (after Martin 1987)

	Biotite	Hornblende	Plagioclase		Magnetite	Ilmenite
			An_{25}	An_{37}		
SiO_2	36.34	42.5	62.26	59.38		
TiO_2	2.74	1.64				50
Al_2O_3	20.22	13.6	23.87	25.65		
Fe_2O_3 + MgO	30.5	27.38			100	50
CaO	0.04	12.29	4.99	7.3		
Na_2O	0.36	2.02	8.58	4.69		
K_2O	9.72	0.55	0.3	1.74		

360–320 Ma interval thus brackets the main tectonothermal activity in the Getic basement. The 325–320 Ma Ar–Ar ages of hornblende and muscovite from the Getic basement (Dallmeyer et al. 1998) indicate cooling rates at 10 ± 5°/myr (Medaris et al. 2003), and unroofing of the granitoids plutons was completed by 310–305 Ma, as Westphalian–Stephanian conglomerates are preserved at the bottom of the sedimentary series covering the Getic basement in the Banat area. The intrusion of the Poniasca (311 ± 2 Ma) pluton thus follows the subduction stage HP metamorphism and the collisional nappe stacking and announces the forthcoming extensional basins.

This story fits well to the end of the evolution of the European Variscan belt. In the Moldanubian (Bohemian massif), the high-pressure and high-temperature metamorphism (HP–HT; 15–20 kbar; 900–1000°C; O'Brien 2000 and references therein) is dated at 340± 316 Ma and is followed by rapid exhumation accompanied by a high-temperature metamorphism ending at c. 330 Ma (Dallmeyer et al. 1992). A catastrophic crustal melting event occurred at 330 Ma and was followed by decreasing heat flow and melt production (Henk et al. 2000) giving rise, in the South Bohemia batholith, to granitoids dated between 327± 1 and,16± 1 Ma (U–Pb zircon; Gerdes et al. 2003). A second increase of the heat flow led to the generation of late Variscan I-type granodiorites (310–290 Ma; Finger et al. 1997); it is considered as a distinct second phase (Henk et al. 2000). The first phase can be correlated to the development of the Saxo-Thuringian belt marked by two successive thrust events. The first occurred during the Saxo-Thuringian-Tepla-Barrandian collision (340–320 Ma) and the second during the Saxo-Thuringian-Rheno-Hercynian collision that ended at c. 310 Ma (Krawczyk et al. 2000). We could with advantage refer, following Cavazza et al. 2004, to (1) a Variscan orogeny

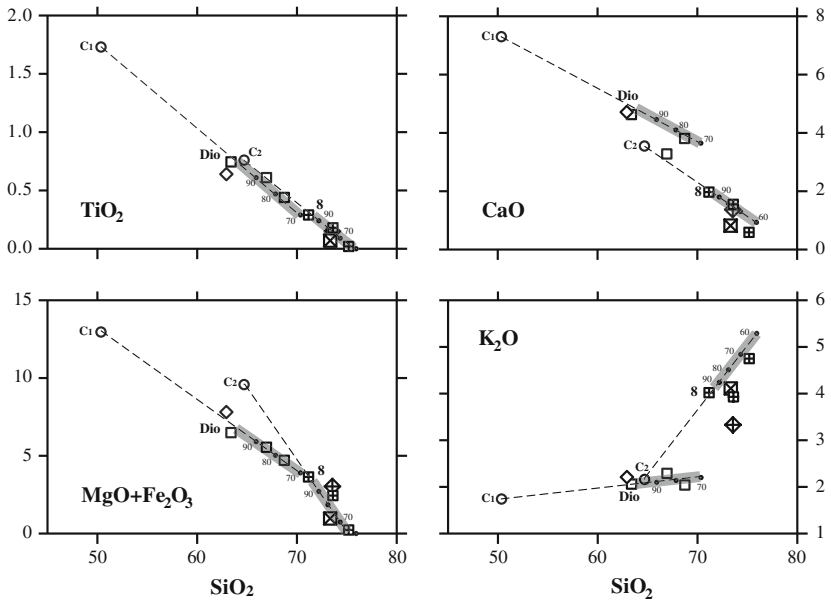

Fig. 8 Major element modelling of the two rock series. Data from Table 6. Same symbols as in Fig. 5. Cumulate C_1 is subtracted from average biotite diorite Dio (average of sample# 4 and #5) to produce a linear liquid line of descent with F values from 90 to 70. Cumulate C_2 is subtracted from granite composition#8 to produce the granitic liquid line of descent (F from 90 to 60). Both cumulate compositions C_1 and C_2 are calculated by mass balance (see text)

Table 6 Chemical and modal compositions of the cumulates extracted from dioritic melt (C_1) and granitic melt (C_2)

	C1 (diorite)	C2 (granite)
SiO_2	50.36	64.7
TiO_2	1.73	0.76
Al_2O_3	21.22	15.46
Fe_2O_3 + MgO	12.96	9.58
CaO	7.3	3.55
Na_2O	4.69	3.8
K_2O	1.74	2.16
R^2	0.069	0.806
(1-F) × 100	26.39	35.47
Interval	1 to 30	1 to 40
Biotite	11.54	20.24
Hornblende	22.17	12.37
Magnetite	2.31	
Ilmenite	2.11	
Plag An_{37}	61.87	
Plag An_{25}		40.57
Quartz		26.82

with the collisional climax between the Hunic and Hanseatic terranes with Laurussia at c. 340 Ma followed by a period of lateral displacement accompanied by major plutonism and (2) an Alleghenian orogeny with the collisional climax between Gondwana and Laurentia at c. 300 Ma, also followed by an important magmatic event attaining the Early Permian.

The Sichevita–Poniasca pluton of crustal origin, following a HP–LT and a HT–LP metamorphism and dated at 311± 2 Ma, can thus be placed at the end of this first Variscan phase. The second Variscan phase is not known in South Carpathians. The Sichevita–Poniasca age range is also known in Bulgaria where granites have been dated at 312–303 Ma (U–Pb zircon), intruding a c. 335 Ma metamorphic basement (Carrigan et al. 2005; 2006), as well as in the Iberian massif where numerous granites intruded between 320 and 306 Ma; a younger set intruded also between 295 and 280 Ma (Fernandez-Suarez et al. 2000; Dias et al. 1998). The Aar massif, in the Alps, developed a similar evolution with older granitoids in the 335–330 Ma range, three plutons at 310± 3 Ma and younger granites at 298± 3 Ma (Schaltegger and Corfu 1992).

This review indicates that the Sichevita–Poniasca pluton belongs to a post-collisional phase of regional scale even if some diachronism is likely, especially between the central and the peripheral parts of the Variscan orogen (Carrigan et al. 2005) and can be considered as having intruded during the very final stage of the Variscan orogeny, the younger plutons found elsewhere being considered as

Table 7 REE and other trace element partition coefficients between mineral and melt used for fractional crystallization calculations (after Martin 1987)

	Hornblende	Ilmenite	Plagioclase	Magnetite	Biotite	Allanite	Apatite	Zircon
La	0.74	0.005	0.4	0.22	0.34	960	25	2
Ce	1.52	0.006	0.27	0.26	0.33	940	35	2.64
Nd	4.26	0.0075	0.21	0.3	0.28	750	58	2.2
Sm	7.77	0.01	0.13	0.35	0.26	620	64	3.14
Eu	3	0.007	1.15	0.26	0.24	56	30	3.14
Gd	10	0.021	0.097	0.28	0.26	440	64	12
Dy	13	0.028	0.064	0.28	3.2	200	58	101.5
Er	14	0.035	0.055	0.22	3.7	100	40	135
Yb	13	0.075	0.049	0.18	4.4	54	22	527
Rb	6	0.1	0.046	0.18	0.062	41	16	345
Ba	0.022		4.4		0.1		2	
K	0.08		0.17	0.96	1.6			
Nb	12		0.055		0.16	100		140
Sr	0.014		2		3			
Zr	0.044		0.5		2		0.01	3800
Ti	7	7	0.04	1.5	0.9			
Y	13		0.01		2	1		3800
V	12	4.5	0.38	8.6	10	28		
Cr	10	8.3	0.01	8.6	25	30		
Co	1.3		0.025		1	2		25
Ni	10	5.9	0.1	9.5	25	28	0.2	

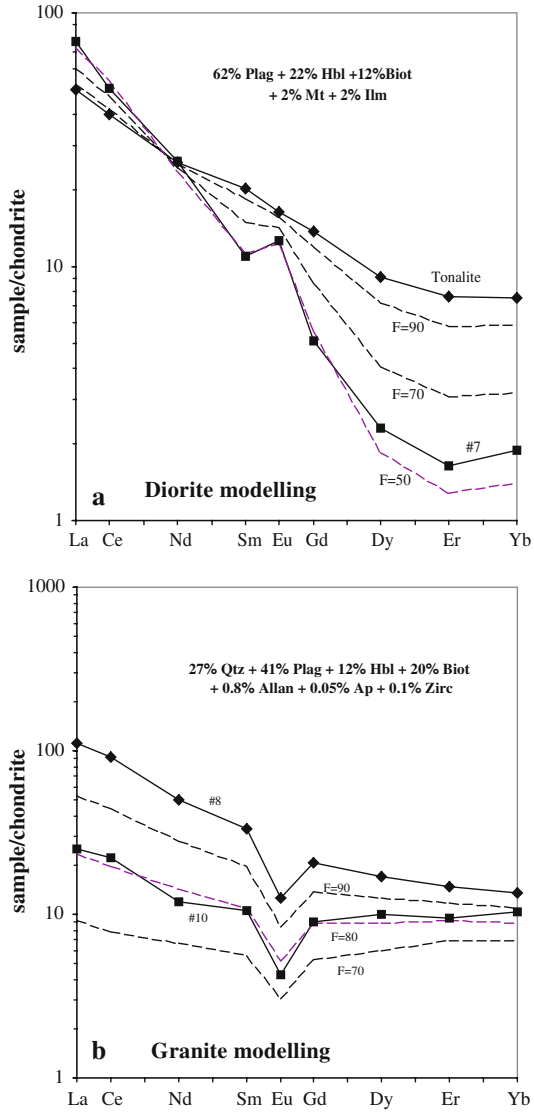

Fig. 9 Chondrite-normalised REE distributions in the trace element modelling of **a** the biotite diorites and **b** the granites. The modal composition of the cumulates C_1 and C_2 result from the major element model (Table 6). The partition coefficients used in the modelling are given in Table 7

Alleghenian rather than Variscan (Cavazza et al. 2004). A common constraint to the numerous geodynamic models invoked to account for the high heat flow is to reduce the thickness of the lithospheric mantle while keeping a thick crust (Henk et al. 2000). Delamination of the lithospheric mantle (or a part of it) following a slab break off induced by the collision (Liégeois et al. 1987; Davies and von Blankenburg 1995) is a viable mechanism for the central part of the Variscan orogen (Henk et al. 2000). This is also a possibility for the Sichevita–Poniasca pluton; however, considering the much smaller amount of granitic melts produced in the Getic nappe, their late age and their alignment along a linear structural trend, thermal relaxation and heat transfer along a lithospheric discontinuity can also be proposed (Liégeois et al. 1998), maybe following a linear lithospheric delamination along these shear zones (Liégeois et al. 2003). The high heat flow along this lithospheric shear zone can have triggered partial melting of the diverse Getic basement components, leading inevitably to heterogeneous magma types. The Sichevita–Poniasca would have intruded during the transcurrent movements generally occurring after a collision and typical of the post-collisional period (Liégeois 1998).

Conclusions

The intrusion of the Poniasca pluton and by implication of the Sichevita pluton, is well dated at 311± 2 Ma on magmatic zircons, and this age is similar to post-collisional granitoid ages elsewhere in the waning stages of the Variscan orogen. This post-collisional status agrees with the metamorphic ages recorded in the Getic metamorphic basement between 360 and 320 Ma. Some U–Pb data obtained on zircon relic cores point to an age of 891 ± 20 Ma, probably corresponding to an ancient component of the magma source also depicted by the two-stage Nd model ages between 850 and 1,350 Ma.

Though displaying a continuous trend of major element compositions from biotite diorite to granite, the Sichevita–Poniasca lithologies do not constitute a unique rock series differentiated from a single parent magma. A hybridization process between two magmas, as suggested by linear relationships in Harker diagrams, does not account for the observed trends of some trace elements. Sr and Nd isotopes and trace elements show in fact that both plutons were formed from several magma batches and that fractional crystallization was the most likely differentiation process explaining the variety of rocks. The Sichevita and Poniasca plutons show that, in a post-collisional setting, heterogeneous crustal sources may have produced at the same time several melt compositions depending on the nature of the melted rocks. Paradoxically some dioritic melts can derive from a source showing a more crustal isotopic character than some granitic melts which can originate from more juvenile material.

This view is supported by the observation that the area is made up of a series of nappes of various ages, metamorphic grades and compositions (Medaris et al. 2003), including both oceanic and continental material (Iancu et al. 1998; Sabau and Massone 2003). It is thus not surprising to get distinct melts and even granites more juvenile than diorites. It only depends on the relative age and nature of the source protoliths. The geodynamical setting is constrained by the necessity of having sufficient heat to melt this crustal source. Combined with the regional context, this is

achieved by calling a higher heat flow along the shear zone along which the Sichevita–Poniasca pluton intruded, during its functioning in post-collisional setting.

This demonstrates that deciphering the origin of granitoids demands a minimum knowledge of the basement. It also shows that a detailed geochemical study is a powerful tool to decipher the geodynamical setting of granitoids but only if it is coupled with other methods. The geochemistry of granitoids results from the composition of their source and melting conditions, not from their geodynamical setting. The latter can be deciphered only by combining field observation, geochronological and geochemical data as well as considerations at the scale of the orogenic belt.

Acknowledgments This study is part of a research programme supported by the European Community (CIPA CT93 0237- DG12 HSMU) and the Belgian CGRI. M.T. was a post-doctorate fellow of the Belgian FNRS at the University of Liège. G. Bologne has helped with the chemical analyses. B. Bonin has kindly provided judicious comments. S. Jung and F. Neubauer are greatly thanked for their constructive reviews.

Appendix: Methods

Zircon grains were hand selected and mounted in epoxy resin, together with chips of the TEMORA (Middledale Gabbroic Diorite, New South Wales, Australia, age= 417 Ma, Black et al. 2003) and 91500 (Geostandard zircon, age= 1,065 Ma, Wiedenbeck et al. 1995) reference zircons. The grains were sectioned approximately in half and polished. Each analysis consisted of five scans through the mass range; the spot diameter was about 18 μm and the primary beam intensity about 4 nA. The data were reduced in a manner similar to that described by Williams (1998) and references therein), using the SQUID Excel Macro of Ludwig (2000). The Pb/U ratios were normalised relative to a value of 0.0668 for the $^{206}Pb/^{238}U$ ratio of the TEMORA zircon, equivalent to an age of 416.75 Ma (Black and Kamo 2003). Uncertainties given for individual analyses (ratios and ages) in Table 1 are at the one σ level, whereas uncertainties in calculated concordia ages are reported at the 2σ level.

Whole-rock analyses were performed by XRF on an ARL 9400 XP spectrometer. The major elements were analysed on lithium tetra- and metaborate glass discs (FLUORE-X65®), with matrix corrections following the Traill-Lachance algorithm. Trace elements (Sr, Rb, Nb, Ni, Zn, and Cu) were measured on pressed pellets and corrected for matrix effects by Compton peak monitoring.

Selected samples were analysed for REE, Y, U, Th, Zr, Hf, Nb, Ba, Ta and Ga by ICP-MS on a VG Elemental Plasma Quad PQ2 after alkali fusion, following the method described in Vander Auwera et al. (1998).

Sr and Nd isotopic compositions were made at the Université Libre de Bruxelles on a Micromass GV Sector 54 multicollector mass spectrometer. The average $^{87}Sr/^{86}Sr$ ratio of the NBS SRM987 standard and $^{143}Nd/^{144}Nd$ ratio of the Rennes Nd standard during the period of analyses were 0.710271 ± 10 ($2\sigma_m$ on 8 measurements) and 0.511971 ± 9 (on 12 measurements), respectively. Sample ratios have been standardised to a value of 0.710250 for NBS987 and to 0.511963 for the Merck standard (corresponding to a La Jolla value of 0.511858).

References

Beard JS, Lofgren GE (1991) Dehydration melting and water saturated melting of basaltic and andesitic greenstones and amphibolites at 1, 3 and 6.9 kbar. J Petrol 32:365–402

Berza T (1997) A hundred years of tectonic studies in South Carpathians: the state of the art. In: Grubic A, Berza T (eds) Geology of Djerdap Area. Geoinstitut, Belgrade, pp 271–276

Birlea L (ed.) (1977) L'importance des minéraux accessoires pour les recherches géologiques et métallogéniques dans les massifs granitoïdes. Annales Université Jean-Bedel Bokassa, 2, Empire Centrafricain

Birlea L (1976) Studiul mineralelor accessorii din masivul granitoid de Sichevita (muntii Almajului) (abstract of Doctorate thesis). University of Bucharest, pp 1–24

Black LP, Kamo SL (2003) TEMORA 1: a new zircon standard for U–Pb geochronology. Chem Geol 200:155–170

Carrigan C, Mukasa S, Haydoutov I, Kolcheva K (2005) Age of Variscan magmatism from the Balkan sector of the orogen, central Bulgaria. Lithos 82:125–147

Carrigan C, Mukasa S, Haydoutov I, Kolcheva K (2006) Neoproterozoic magmatism and Carboniferous high-grade metamorphism in the Sredna Gora Zone, Bulgaria: an extension of the Gondwana-derived Avalonia–Cadomian belt? Precambrian Res 147:404–416

Cavazza W, Roure FM, Spakman W, Stampfli GM, Ziegler PE (2004). The TRANSMED Atlas—the Mediterranean region from Crust to Mantle. Springer, Heidelberg, 141 pages + 1 CD-ROM

Chappell BW, White AJR (1974) Two contrasting granite types. Pac Geol 8:173–174

Chappell BW, White AJR (1991) Restite enclaves and the restite model. In: Didier J, Barbarin B (eds) Enclaves and granite petrology. Elsevier, Amsterdam, pp 375–381

Chappell BW, White AJR, Wyborn D (1987) The importance of residual source material (restite) in granite petrogenesis. J Petrol 28: 1111–1138

Dallmeyer RD, Neubauer F, Höck V (1992) Chronology of late Palaeozoic tectonothermal activity in the southeastern Bohemian massif, Austria (Moldanubian and Moravo-Silesian zones): $^{40}Ar/^{39}Ar$ mineral age controls. Tectonophysics 210:135–153

Dallmeyer RD, Neubauer F, Fritz H, Mocanu V (1998) Variscan versus Alpine tectonothermal evolution of the southern Carpathian orogen: constraints from $^{40}Ar/^{39}Ar$ ages. Tectonophysics 290:111–135

Davies JH, von Blankenburg F (1995) Slab breakoff: a model of lithospheric detachment and ist test in the magmatism and deformation of collisional orogens. Earth Planet Sci Lett 129:85–102

Dias G, Leterrier J, Mendes A, Simoes PP, Bertrand JM (1998) U-Pb zircon and monazite geochronology of post-collisional Hercy-

nian granitoids from the Central Iberian Zone (northern Portugal). Lithos 45:349–369
Didier J, Barbarin B (1991) Enclaves and granite petrology. Development in Petrology 13. Elsevier, Amsterdam, p 625
Debon F (1991) Comparative major element chemistry in various ''microgranular enclave-plutonic host'' pairs. In: Didier J, Barbarin B (eds) Enclaves and granite petrology. Elsevier, Amsterdam, pp 293–312
Dragusanu C, Tanaka T (1997) 1.57 Ga magmatism in the South Carpathians; implications for the pre-Alpine basement and evolution of the mantle under the European continent. J Geol 107:237–248
Duchesne JC, Wilmart E (1997) Igneous charnockites and related rocks from the Bjerkreim-Sokndal layered intrusion (Southwest Norway): a jotunite (hypersthene monzodiorite)-derived A-type granitoids suite. J Petrol 38:337–369
Fenner CN (1926) The Katmai magmatic province. J Geol 34:673–772
Fernando-Suarez J, Dunning GR, Jenner GA, Gutiérrez-Alonso G (2000) Variscan collisional magmatism and deformation in NW Iberia: constraints from U–Pb geochronology of granitoids. J Geol Soc London 157: 565–576
Finger F, Roberts MP, Haunschmid B, Schermaier A, Steyrer HP (1997) Variscan granitoids of Central Europe: their typology, potential sources and tectonothermal relations. Mineral Petrol 61:67–96
Frost BR, Barnes CG, Collins WJ, Arculus RJ, Ellis DJ, Frost CD (2001) A geochemical classification for granitic rocks. J Petrol 42: 2033–2048
Gerdes A, Friedl G, Parrish RR, Finger F (2003) High-resolution geochronology of Variscan granite emplacement—the South Bohemian batholith. J Czech Geol Soc 48:53–54
Harrison TM, Watson EB (1984) The behavior of apatite during crustal anatexis: equilibrium and kinetic considerations. Geochim Cosmochim Acta 48:1467–1477
Helz R (1976) Phase relations of basalt in their melting ranges at $PH_2O = 5$ kb. Part 2. Melt compositions. J Petrol 17:139–193
Henk A, von Blankenburg F, Finger F, Schaltegger U, Zulauf G (2000) Syn-convergent high-temperature metamorphism and magmatism in the Variscides: a discussion of potential heat sources. In: Franke W, Haak V, Oncken O, Tanner D (eds) Orogenic processes: quantification and modelling in the Variscan belt. Geological Society, London, Special Publication, 179:387–399
Holtz F, Johannes W (1991) Genesis of peraluminous granites I. Experimental investigation of melt composition at 3 and 5 kb and various H_2O activities. J Petrol 32:935–958
Iancu V (1998) Relatii intre granitoide si metamorfite pre-alpine in Carpathii Meridionale (in romanian). Doctorat dissertation Thesis, University of Bucharest, p 206
Iancu V, Andar P, Tatu M (1996) The late Variscan Sichevita–Poniasca granitoids: petrochemical polarity and tectonically controlled emplacement of the magma. Inst Geol Rom 69(suppl. n1): 103–106
Iancu V, Balintoni I, Sabau G (1988) Variscan tectonic units from the Getic Domain, Bozovici Zone. DS Inst Geol Geofiz 72–73:153–161
Iancu V, Berza T, Seghedi, A, Gheuca, I, Hann HP (2005a) Alpine polyphase tectono-metamorphic evolution of the South Carpathians: a new overview. Tectonophysics 410:337–365
Iancu V, Berza T, Seghedi A, Maruntiu M (2005b) Palaeozoic rock assemblages incorporated in the South Carpathian Alpine thrust belt (Romania and Serbia): a review. Geol Belg 8:48–68
Iancu V, Maruntiu M (1989) Toronita Zone and problems of the Pre-Alpine metamorphic basement of the Getic and Danubian realms. DS Inst Geol Geofiz 71:223–237
Iancu V, Maruntiu M, Johan V, Ledru P (1998) High-grade metamorphic rocks in the pre-Alpine nappe stack of the Getic–Supragetic basement (Median Dacides, South Carpathians, Romania). Mineral Petrol 63:173–198
Jung S, Hoernes S, Mezger K (2002) Synorogenic melting of mafic lower crust: constraints from geochronology, petrology and Sr, Nd, Pb and O isotope geochemistry of quartz diorites (Damara orogen, Namibia). Contrib Mineral Petrol 143:551–566
Krawczyk CM, Stein E, Choi S, Oettinger G, Schuster K, Götze HJ, Haak V, Oncken O, Prodehl C, Schulze A (2000) Geophysical constraints on exhumation mechanisms of high pressure rocks: the Saxo–Thuringian case between the Franconian line. In: Franke W, Haak V, Oncken O, Tanner D (eds) Orogenic processes: quantification and modelling in the Variscan belt. Geological Society, London, Special Publication, 179:303–322
Ledru P, Cocherie A, Iancu V, Maruntiu M (1997) The gneissic units of the Median Dacides (Getic–Supragetic Domain): an exotic segment of the European Variscides. Rom J Mineral 78 (suppl. 1): 48–49 (Abstract volume, 4th National Symposium on Mineralogy, 3–8 October, Iasi)
Liégeois JP (1998) Preface—some words on the post-collisional magmatism. Lithos 45:XV–XVII
Liégeois JP, Bertrand J, Black R (1987) The subduction- and collision-related Pan-African composite batholith of the Adrar des Iforas (Mali): a review. Geol J 22:185–211
Liégeois JP, Navez J, Hertogen J, Black R (1998) Contrasting origin of post-collisional high-K calc-alkaline and shoshonitic versus alkaline and peralkaline granitoids. The use of sliding normalization. Lithos 45:1–28
Liégeois JP, Latouche L, Boughrara M, Navez J Guiraud M (2003) The LATEA metacraton (Central Hoggar, Tuareg shield, Algeria): behaviour of an old passive margin during the Pan-African orogeny. J Afr Earth Sci 37:161–190
Ludwig KR (2000) SQUID 1.00: a user's manual. Berkeley Geochronol Cent Spec Publ 2:1–19
Martin H (1987) Petrogenesis of Archaean trondhjemites, tonalites and granodiorites from Eastern Finland: major and trace element geochemistry. J Petrol 28:921–953
Maruntiu M, Iancu V, Alexe V, Stoian M (1996) - Geochemistry of the metamagmatic rocks in the Getic–Supragetic Domain of the South Carpathians. Inst Geol Roman 69:225–228
McDermott F, Harris NBW, Hawkesworth CL (1996) Geochemical constraints on crustal anatexis: a case study from the Pan-African Damara granitoids of Namibia. Contrib Mineral Petrol 123:406–423
Medaris GJ, Ducea M, Ghent E, Iancu V (2003) Conditions and timing of high-pressure Variscan metamorphism in the South Carpathians, Romania. Lithos 70:141–161
Millisenda CC, Liew TC, Hofman AW, Köhler H (1994) Nd isotopic mapping of the Sri Lanka basement: update and additional constraints from Sr isotopes. Precambrian Res 66:95–110
Murgoci (1905) Sur l'existence d'une grande nappe de recouvrement dans les Karpathes Méridionales. CR Acad Sci Paris 31 Juillet 1905
O'Brien PJ (2000) The fundamental Variscan problem: high-temperature metamorphism at different depths and hig-pressure metamorphism at different temperatures. In: Franke W, Haak V, Oncken O, Tanner D (eds) Orogenic processes: quantification and modelling in the Variscan belt. Geological Society, London, Special Publication, 179, 369–386
Peccerillo R, Taylor SR (1976) Geochemistry of Eocene calc-alkaline volcanic rocks from the Kastamonu area, northern Turkey. Contrib Mineral Petrol 58:489–502
Pitcher WS (1987) Granites and yet more granites fourty years on. Geol Rundsch 76:51–79

Rapp RP, Watson EB (1995) Dehydration melting of metabasalt at 8–32 kbar: implications for continental growth and crust-mantle recycling. J Petrol 36:891–932

Roberts MP, Clemens JD (1993) Origin of high-potassium, calc-alkaline, I-type granitoids. Geology 21:825–828

Rushmer T (1991) Partial melting of two amphibolites: contrasting experimental results under fluid absent conditions. Contrib Mineral Petrol 107:41–59

Sabau G, Massone HJ (2003) Relationships among eclogite bodies and host rocks in the Lotru metamorphic suite (South Carpathians, Romania): petrological evidence for multistage tectonic emplacement of eclogites in a medium-pressure terrain. Int Geol Rev 45: 225–262

Sandulescu M, Krautner HP, Borcos M, Nastaseanu S, Patrulius D, Stefanescu M, Ghenea C, Lupu M, Savu H, Bercia I, Marinescu F (1978) Geological map of Romania, scale 1:1,000,000

Savu H, Tiepac I, Udrescu C (1997) A comparative study of two granitoid series (Poneasca and Buchin) from the Semenic Mountains—Southern Carpathians. Stud Cercet Geol 42:13–28

Savu H, Vasiliu C (1969) Contributii la cunoatterea structurii si chimismului masivului granitoid de la Poniasca (Muntii Semenic). DS Inst Geol Buchuresti 54:383–487

Seghedi A, Berza T (1994) Duplex interpretation for the structure of the Danubian thrust sheets. Rom J Tect Reg Geol 75:57

Schaltegger U, Corfu F (1992). The age and source of Late Hercynian magmatism in the central Alps: evidence from precise U–Pb ages and initial Hf isotopes. Contrib Mineral Petrol 111:329–344

Stan N, Intorsureanu I, Tiepac I, Udrescu C (1992) Petrology of the Sichevita granitoids (South Carpathians). Rom J Petrol 75:1–15

Stan N, Tiepac I (1994) Characterization of S-I type granitoids from the Banat area, South Carpathians. Rom J Petrol 76:33–39

Stefanescu M (ed) (1988) Geological cross-sections at scale 1:200,000. Inst Geol Geofiz, Buchuresti

Taylor SR, McLennan, SM (1985) The continental crust: its composition and evolution. Blackwell, Oxford, p 312

Vander Auwera J, Bologne G, Roelandts I, Duchesne JC (1998) Inductively coupled plasma-mass spectrometry (ICP-MS) analysis of silicate rocks and minerals. Geol Belg 1:49–53

Vaskovic N, Christofides G, Koroneos A, Sreckovic-Batocanin D, Milovanovic D (2004) Mineralogy and petrology of the Brnjica granitoids (Eastern Serbia). Bull Geol Soc Greece 36:615–624

Vaskovic N, Matovic V (1997) The Hercynian granitoids of Djerdap (North–East Serbia), International Symposium, Geology of the Danube Gorges, Donj Milanovac, pp 129–140

Watson EB, Harrison TM (1983) Zircon saturation revisited: temperature and compositional effects in a variety of crustal magma types. Earth Planet Sci Lett 64:295–304

Wiedenbeck M, Allé P, Corfu F, Griffin WL, Meier M, Oberli F, Von Quadt A, Roddick JC, Spiegel W (1995) Three natural zircon standards for U–Th–Pb, Lu–Hf, trace element and REE analyses. Geostandards Newsl 19:1–23

Williams IS (1998) U–Th–Pb Geochronology by ion microprobe. In: McKibben MA, Shanks III WC, Ridley WI (eds) Applications of Microanalytical Techniques to Understanding Mineralising Processes. Rev Econ Geol 7:1–35